Conformational Behavior of Tris(pentafluorophenyl)borane−Benzotriazole Adducts

Francesca Focante,[†,1] Rino Leardini,[†] Andrea Mazzanti,*[†] Pierluigi Mercandelli,[‡] and Daniele Nanni[†]

Dipartimento di Chimica Organica "A. Mangini", Università di Bologna, viale Risorgimento 4, I-40136 Bologna, Italy, and Dipartimento di Chimica Strutturale e Stereochimica Inorganica, Università di Milano, via Venezian 21, I-20133 Milano, Italy

The stereomutations in a class of tris(pentafluorophenyl)borane−benzotriazole adducts are investigated by means of variable-temperature ^{19}F NMR and X-ray crystallography. At low temperature the presence of a pair of conformational enantiomers is confirmed by NMR spectra obtained in a chiral medium. Two different energy barriers, corresponding to an enantiomerization process and a B−N rotation, were observed and their values measured ($\Delta G^{\ddagger} = 10.7$ and 12.8 kcal mol^{-1} in the case of **1**). In the case of the bis-adduct **3**, two conformational diastereoisomers with different populations were detected at low temperature, while only one diastereoisomer is present in the crystalline state.

Introduction

In recent years there has been an increasing interest in the chemistry of pentafluorophenyl boranes because of their enhanced Lewis acidity, similar to the extremely moisture-sensitive and volatile gaseous BF_3. The Lewis acidity of $B(C_6F_5)_3$ can be converted into Brønsted acidity by complexation with water, alcohols, imines, secondary amines, or nitrogen-heterocycles, and the corresponding adducts are an attractive alternative as cocatalysts in the homogeneous Ziegler−Natta olefin polymerization.[2]

Together with the preparation and the analysis of the chemical properties of these adducts, several studies have recently been carried out by means of low-temperature NMR and X-ray diffraction in order to study their conformational properties.[3−8] In some cases the energy barriers for internal motion of the pentafluorophenyl groups were measured, but, to the best of our knowledge, it was not until the recent paper by Resconi, Beringhelli, et al.[3] that a thorough mechanistic interpretation of the dynamics of the perfluorinated borate moiety was proposed.

In this paper we gain more insight into the structural and conformational properties of perfluorinated aryl borates by expanding our study to include the adducts of $B(C_6F_5)_3$ with benzotriazole. The ability of benzotriazole to react with $B(C_6F_5)_3$ in a 1:1 or 1:2 ratio to give, respectively, a mono- or a bis-substituted adduct allows us to analyze more deeply the conformational behavior of these compounds, with the aim of obtaining a full rationale of the molecular stereodynamics.

Results and Discussion

Adduct **1** was readily prepared in quantitative yield by reaction of benzotriazole with $B(C_6F_5)_3$ in dichloromethane at room temperature. Adducts **2** and **3** were prepared in one step by treating benzotriazole with $B(C_6F_5)_3$ (1 equiv for **2** and 2 equiv for **3**[9]) and triethylamine in dichloromethane at room temperature. All the adducts are stable both in air and in solution (acetone, toluene, dichloromethane), with no decomposition byproducts detected after several weeks.

The three adducts were tested as catalysts for the homopolymerization of liquid 1-hexene, and the preliminary data indicate that adduct **3** is more efficient with respect to **1** and **2** (see Supporting Information).[10]

From an extensive search of the Cambridge Structural Database (CSD) it can be seen that tetrasubstituted perfluoroaryl borates usually adopt a distorted tetrahedral conformation around the boron atom. Depending on the nature of the four aryl substituents, the structures can be classified in terms of the "*n*-blade propeller" terminology proposed by Mislow.[11] In the case

* To whom correspondence should be addressed. Phone: +39 051 2093633. Fax: +39 051 2093654. E-mail: mazzand@ms.fci.unibo.it.
† Università di Bologna.
‡ Università di Milano.

(1) In partial fulfillment for the Ph.D. in Chemical Sciences, University of Bologna. Current address: Basell Polyolefins, Centro Ricerche "Giulio Natta", P.le Donegani 12, I-44100 Ferrara, Italy.

(2) Marks, T. J. *Acc. Chem. Res.* **1992**, *25*, 57−65. Yang, X.; Stern, C. L.; Marks, T. J. *J. Am. Chem. Soc.* **1994**, *116*, 10015. Erker, G. *Dalton Trans.* **2005**, *11*, 1883−1890. Li, L.; Stern, C. L.; Marks, T. J. *Organometallics* **2000**, *19*, 3332−3337. Li, L.; Marks, T. J. *Organometallics* **1998**, *17*, 3996−4003. Sun, Y.; Metz, M. V.; Stern, C. L.; Marks, T. J. *Organometallics* **2000**, *19*, 1625−1627. Chen, E. Y.-X.; Marks, T. J. *Chem. Rev.* **2000**, *100*, 1391−1434.

(3) Guidotti, S.; Camurati, I.; Focante, F.; Angellini, L.; Moscardi, G.; Resconi, L.; Leardini, R.; Nanni, D.; Mercandelli, P.; Sironi, A.; Beringhelli, T.; Maggioni, D. *J. Org. Chem.* **2003**, *68*, 5445−5465, and references therein.

(4) Focante, F.; Camurati, I.; Nanni, D.; Leardini, R.; Resconi, L. *Organometallics* **2004**, *23*, 5135−5141.

(5) Beringhelli, T.; D'Alfonso, G.; Donghi, D.; Maggioni, D.; Mercandelli, P.; Sironi, A. *Organometallics* **2003**, *22*, 1588−1590.

(6) Blackwell, J. M.; Piers, W. E.; Parvez, M.; McDonald, R. *Organometallics* **2002**, *21*, 1400−1407.
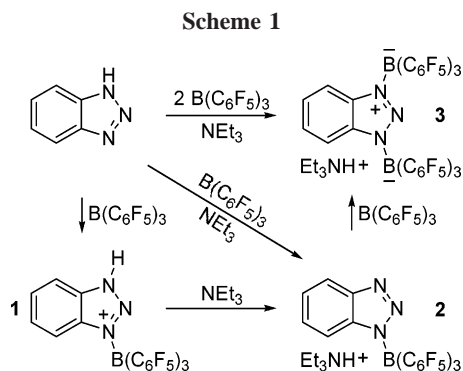
(7) Fraenk, W.; Klapötke, T. M.; Krumm, B.; Mayer, P.; Piotrowski, H.; Vogt, M. *Z. Anorg. Allg. Chem.* **2002**, *628*, 745−750.

(8) Vagedes, D.; Erker, G.; Kehr, G.; Bergander, K.; Kaataeva, O.; Frölich, R.; Grimme, S.; Mück-Lichtenfeld, C. *Dalton Trans.* **2003**, 1337−1344.

(9) LaPointe, R. E. (Dow Chemical Company) Int. Pat. Appl. WO 99/42467.

(10) Resconi, L.; Guidotti, S.; Camurati, I.; Frabetti, R.; Focante, F.; Nifant'ev, I. E.; Laishevtsev, I. P. *Macromol. Chem. Phys.* **2005**, *206*, 1405.

(11) This concept was introduced and discussed by Mislow and further illustrated by Glaser. See: Mislow, K. *Chemtracts: Org. Chem.* **1989**, *2*, 151. Glaser, R. In *Acyclic Organonitrogen Stereodynamics*; Lambert, J. B., Takeuchi, Y., Eds.; VCH: New York, 1992; Chapter 4, p 123.
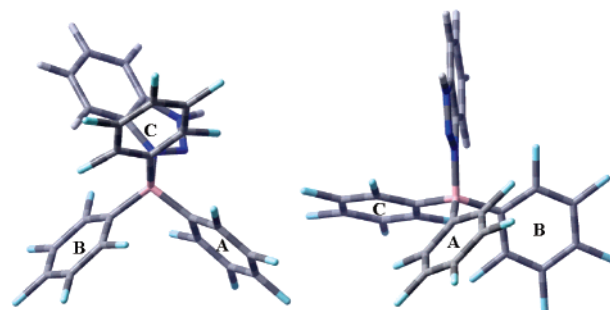
Scheme 1

Figure 1. Optimized structure of **1** (HF/6-31G). Left: projection from the (ring C)−boron−N(benzotriazole) plane. Right: projection from the (ring A)−boron−N(benzotriazole) plane.

Scheme 2

of tris(pentafluorophenyl)borates similar to adduct **1**, X-ray diffraction data[3,5,7,8] indicate that two pentafluorobenzene rings are geared together in a two-blade propeller conformation, while the third one and the heteroaromatic ring (i.e., the fourth substituent) do not participate in the propeller conformation. Thus the structures can be interpreted using the "two-blade propeller" terminology and not with the "three-blade propeller" one. In fact, to produce a three-blade propeller, the fourth substituent has either to be absent or to possess the same C_3 local symmetry.[12] In the compounds that we discuss here the fact that one of the two ungeared rings is identical to the two generating the propeller moiety is important and could modify the whole conformational process.

The dynamics of a two-blade propeller have been analyzed in detail.[13−16] When two aryl groups are connected to a single ligating atom (Ar−X−Ar), they can be considered to be the molecular analogues of a macroscopic two-blade propeller and the internal rotations involving the two Ar−X bonds can be described according to the so-called "cogwheeling circuit". The dynamic enantiomerization process might occur, in principle, via three possible correlated pathways, corresponding to the *n*-ring-flip mechanisms displayed in Scheme 2, where *n* can be equal to 0, 1, or 2.[13]

The zero-ring-flip pathway ($n = 0$) is a conrotatory motion leading to a transition state where both aryl rings are coplanar with the C1−B−C1′ plane. Consequently, the corresponding barrier is expected to be extremely high and unlikely to take place. In any case this process does not imply an exchange of environment for the diastereotopic ortho fluorine atoms and is thus unable to account for the spectral observations, being NMR invisible.[13,16a] The one-ring-flip process ($n = 1$) is a disrotatory motion leading to a transition state where one ring is orthogonal to and the other coplanar with the C1−B−C1′ plane (gear-meshing). This transition state also has a degenerate form where the disposition of the rings is interchanged.[14,15] Finally, the two-ring-flip process ($n = 2$) is a conrotatory motion having a transition state where both rings are orthogonal to the C1−B−
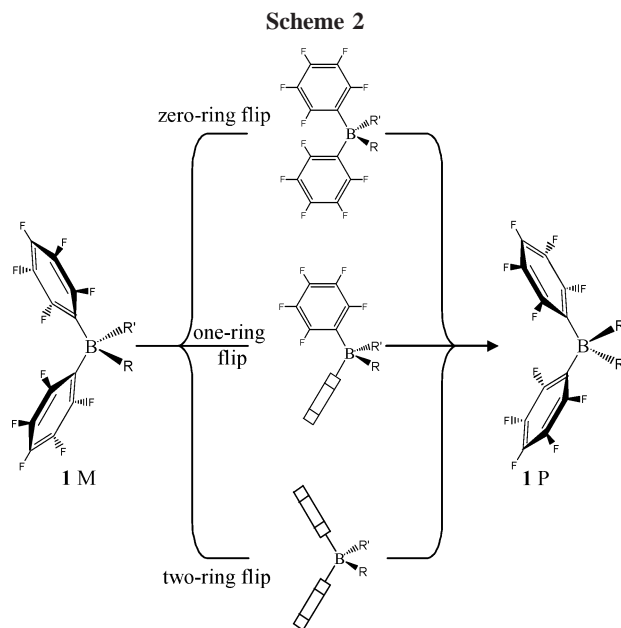
C1′ plane (gear-clashing). The two latter pathways are, in principle, both NMR visible in that they require that the ortho fluorine atoms exchange their positions.[14] All three processes require that the motion of the two rings is correlated, in that the torsion of one ring drives a concomitant torsion of the second one ("cogwheel mechanism").

In the case of adduct **1** we were not able to obtain a good X-ray diffraction structure. Thus the structure reported in Figure 1 was calculated using ab initio methods (HF/6-31G level[17]).

Owing to the presence of the helical conformation generated by rings A and B, the minimum energy structure of compound **1** has C_1 symmetry, and thus a pair of conformational enantiomers is expected when all the rotations around the B−N and

(12) See for example the structures of (a) tris(pentafluorophenyl)borane adducts with triphenylphosphine, acetonitrile, and *p*-nitrobenzonitrile: Jacobsen, H.; Berke, H.; Doering, S.; Kehr, G.; Erker, G.; Froehlich, R.; Meyer, O. *Organometallics* **1999**, *18*, 1724−1735. (b) Trimesityl borane: Blount, J. F.; Finocchiaro, P.; Gust, D.; Mislow, K *J. Am. Chem. Soc.* **1973**, *95*, 7019−7029. (c) Trimesityl methane: Blount, J. F.; Mislow, K. *Tetrahedron Lett.* **1975**, *11*, 909−12.

(13) (a) Mislow, K. *Acc. Chem. Res.* **1976**, *9*, 26. (b) Rappoport, Z.; Biali, S. E. *Acc. Chem. Res.* **1997**, *30*, 307.

(14) Biali, S. E.; Nugiel, D. A.; Rappoport, Z. *J. Am. Chem. Soc.* **1989**, *111*, 846.

(15) Rappoport, Z.; Biali, S. E.; Kaftory, M. *J. Am. Chem. Soc.* **1990**, *112*, 7742.

(16) (a) Grilli, S.; Lunazzi, L.; Mazzanti, A.; Casarini, D.; Femoni, C. *J. Org. Chem.* **2001**, *66*, 488. (b) Grilli, S.; Lunazzi, L.; Mazzanti, A.; Mazzanti, G. *J. Org. Chem.* **2001**, *66*, 748. (c) Casarini, D.; Grilli, S.; Lunazzi, L.; Mazzanti, A. *J. Org. Chem.* **2001**, *66*, 2757.

(17) Frisch, M. J.; Trucks, G. W.; Schlegel, H. B.; Scuseria, G. E.; Robb, M. A.; Cheeseman, J. R.; Montgomery, J. A., Jr.; Vreven, T.; Kudin, K. N.; Burant, J. C.; Millam, J. M.; Iyengar, S. S.; Tomasi, J.; Barone, V.; Mennucci, B.; Cossi, M.; Scalmani, G.; Rega, N.; Petersson, G. A.; Nakatsuji, H.; Hada, M.; Ehara, M.; Toyota, K.; Fukuda, R.; Hasegawa, J.; Ishida, M.; Nakajima, T.; Honda, Y.; Kitao, O.; Nakai, H.; Klene, M.; Li, X.; Knox, J. E.; Hratchian, H. P.; Cross, J. B.; Bakken, V.; Adamo, C.; Jaramillo, J.; Gomperts, R.; Stratmann, R. E.; Yazyev, O.; Austin, A. J.; Cammi, R.; Pomelli, C.; Ochterski, J. W.; Ayala, P. Y.; Morokuma, K.; Voth, G. A.; Salvador, P.; Dannenberg, J. J.; Zakrzewski, V. G.; Dapprich, S.; Daniels, A. D.; Strain, M. C.; Farkas, O.; Malick, D. K.; Rabuck, A. D.; Raghavachari, K.; Foresman, J. B.; Ortiz, J. V.; Cui, Q.; Baboul, A. G.; Clifford, S.; Cioslowski, J.; Stefanov, B. B.; Liu, G.; Liashenko, A.; Piskorz, P.; Komaromi, I.; Martin, R. L.; Fox, D. J.; Keith, T.; Al-Laham, M. A.; Peng, C. Y.; Nanayakkara, A.; Challacombe, M.; Gill, P. M. W.; Johnson, B.; Chen, W.; Wong, M. W.; Gonzalez, C.; Pople, J. A. *Gaussian 03*, revision C.02; Gaussian, Inc.: Wallingford, CT, 2004.
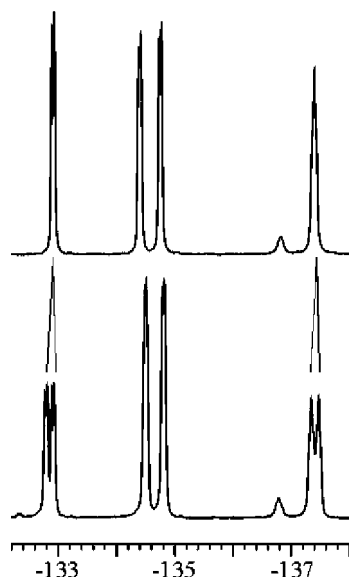
Figure 2. Part of the ortho fluorine region of the ^{19}F NMR spectrum of **1** (564.3 MHz in CD$_2$Cl$_2$). Top: spectrum obtained at -80 °C. Bottom: the same spectrum obtained in the presence of optically pure R-($-$)-2,2,2-trifluoro-1-(9-anthryl)ethanol.

B−C bonds are frozen. Apart from the presence of the benzotriazole cycle, the conformation of the B(C$_6$F$_5$)$_3$ moiety is almost identical to that of other available X-ray crystal structures.[18] One of the rings involved in the two-blade propeller (ring A in Figure 1) forms a dihedral angle with the benzo-triazole ring of about -4°, while the other ring (ring B in Figure 1) forms an angle of -119° (dihedral angles are calculated using the atoms C$_{ipso}$−B−N−N).

The ^{19}F spectrum of **1** at room temperature shows three broad signals corresponding to the ortho, meta, and para fluorine atoms of the three C$_6$F$_5$ rings. When the sample is cooled to -80 °C, the spectrum (obtained in CD$_2$Cl$_2$ and in toluene-d_8) exibits a total of 15 ^{19}F signals corresponding to six ortho, six meta, and three para fluorines. This result confirms that at this temperature all the B−N and B−C rotations are slow on the NMR time scale and that the molecule now has C_1 symmetry, as previously predicted by calculations and also experimentally observed in other cases.[3,8] The existence of a pair of conformational enantiomers was confirmed by acquiring the ^{19}F spectrum at the same temperature (-80 °C) in the presence of an enantio-merically pure medium, such as Pirkle's alcohol.[19] Under these experimental conditions the splitting of some ortho fluorine signals reveals a 50:50 mixture of the two conformational enantiomers (see Figure 2).

On raising the temperature, a complex evolution of the ^{19}F spectra was observed (see Figure 3). Up to -55 °C we still observed three different lines for the para fluorine signals, indicating that the three rings are still diastereotopic. On increasing the temperature, line broadening and coalescence of only two lines was observed, while the third line remained sharp. This fact indicates a fast exchange between two para fluorines (and thus between two C$_6$F$_5$ rings), which does not affect the remaining signal. From the complete line shape simulations the rate constants (indicated by k_{13} in Figure 3) and hence the free energy of activation of the dynamic process ($\Delta G^{\ddagger} = 10.7 \pm$

Figure 3. Left: temperature dependence of the para region of the ^{19}F NMR signals of compound **1** (564.3 MHz in CD$_2$Cl$_2$ apart from the spectrum at $+75$ °C, obtained in C$_2$D$_2$Cl$_4$). Right: line shape simulations obtained with the rate constants indicated.

0.2 kcal mol^{-1}) were obtained.[20] The third line started showing dynamic exchange with the other two only above -26 °C (k_{12} and k_{23} in Figure 3), the effect being most remarkable at -17 °C and above. At $+75$ °C the three signals yielded a single line, indicating that a second dynamic process with a higher energy barrier ($\Delta G^{\ddagger} = 12.8 \pm 0.2$ kcal mol^{-1}) exchanges all three rings.

The same kind of dynamic evolution was observed for the six ortho fluorine signals (see Figure 4): four lines belonging to two rings started the mutual exchange at low temperature (above -36 °C), while the remaining two lines started showing

(18) Focante, F.; Mercandelli, P.; Sironi, A.; Resconi, L. *Coord. Chem. Rev.* **2006**, *250*, 170.

(19) Use was made of enantiopure R-($-$)-2,2,2-trifluoro-1-(9-anthryl)-ethanol; see: Pirkle, W. H.; Sikkenga, D. L.; Pavlin, M. S. *J. Org. Chem.* **1977**, *42*, 384−387.
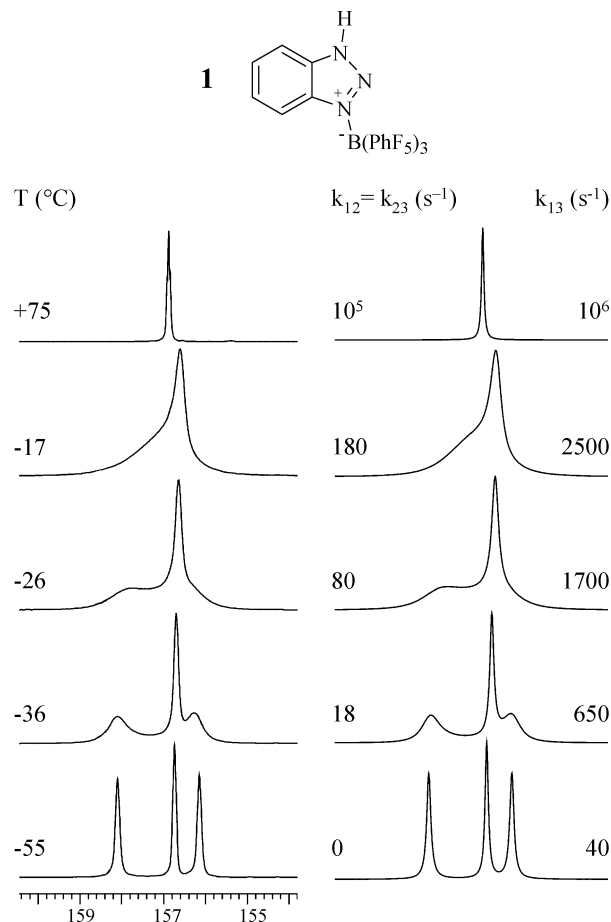
(20) In the restricted temperature range where this dynamic process could be monitored, the free energy of activation was found to be essentially constant within experimental error, suggesting a negligible value for the activation entropy, as often observed in conformational processes. See: Hoogosian, S.; Bushweller, C. H.; Anderson, W. G.; Kigsley, G. *J. Phys. Chem.* **1976**, *80*, 643. Lunazzi, L.; Cerioni, G.; Ingold, K. U. *J. Am. Chem. Soc.* **1976**, *98*, 7484. Bernardi, F.; Lunazzi, L.; Zanirato, P.; Cerioni, G. *Tetrahedron* **1977**, *33*, 1337. Lunazzi, L.; Magagnoli, C.; Guerra, M.; Macciantelli, D. *Tetrahedron Lett.* **1979**, 3031. Cremonini, M. A.; Lunazzi, L.; Placucci, G.; Okazaki, R.; Yamamoto, G. *J. Am. Chem. Soc.* **1990**, *112*, 2915. Anderson, J. E.; Tocher, D. A.; Casarini, D.; Lunazzi, L. *J. Org. Chem.* **1991**, *56*, 1731. Borghi, R.; Lunazzi, L.; Placucci, G.; Cerioni, G.; Foresti, E.; Plumitallo, A. *J. Org. Chem.* **1997**, *62*, 4924. Garcia, M. B.; Grilli, S.; Lunazzi, L.; Mazzanti, A.; Orelli, L. R. *J. Org. Chem.* **2001**, *66*, 6679. Garcia, M. B.; Grilli, S.; Lunazzi, L.; Mazzanti, A.; Orelli, L. R. *Eur. J. Org. Chem.* **2002**, 4018. Casarini, D.; Rosini, C.; Grilli, S.; Lunazzi, L. Mazzanti, A. *J. Org. Chem.* **2003**, *68*, 1815. Casarini, D.; Grilli, S.; Lunazzi, L.; Mazzanti, A. *J. Org. Chem.* **2004**, *69*, 345. Bartoli, G.; Lunazzi, L.; Massacesi, M.; Mazzanti, A. *J. Org. Chem.* **2004**, *69*, 821. Casarini, D.; Coluccini, C.; Lunazzi, L.; Mazzanti, A.; Rompietti, R. *J. Org. Chem.* **2004**, *69*, 5746.
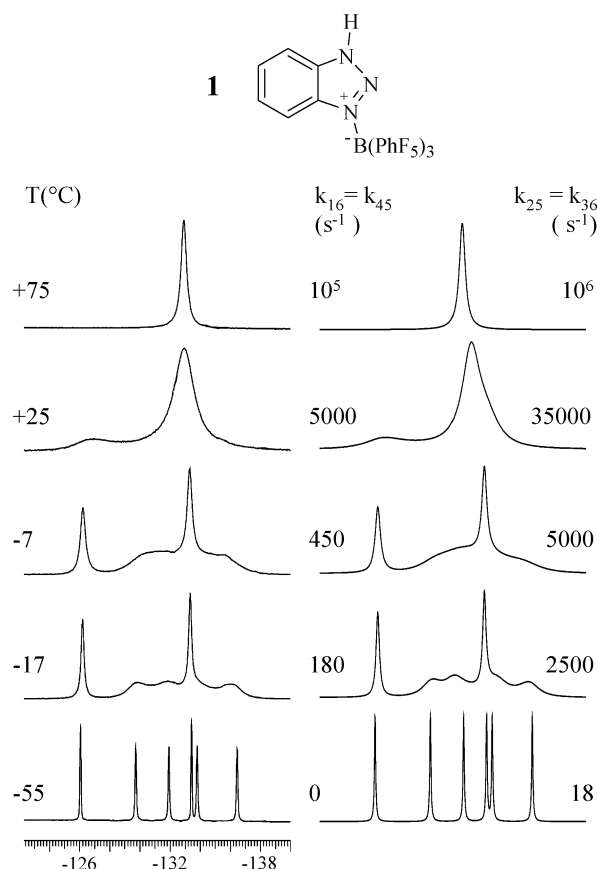
Scheme 3

Figure 4. Left: temperature dependence of the ortho region of the ^{19}F NMR signals of compound **1** (564.3 MHz in CD_2Cl_2 apart from the spectrum at +75 °C, obtained in $C_2D_2Cl_4$). Right: line shape simulations obtained with the rate constants indicated.

dynamic exchange with the others only at higher temperatures (−7 °C). The two energy barriers obtained by line shape simulations are exactly the same obtained by the simulations of the para fluorine signals.[21]
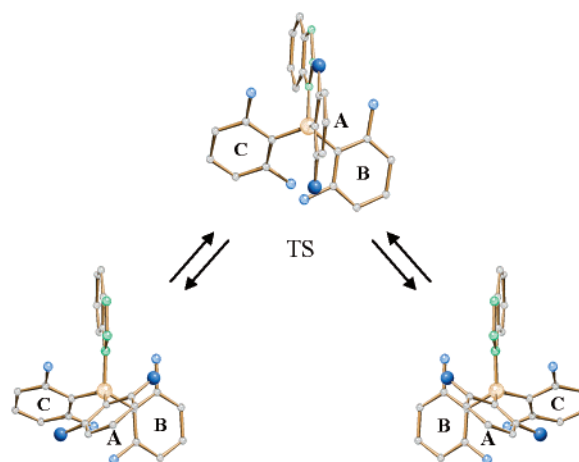
To rationalize the dynamic behavior of the $B(C_6F_5)_3$ group, we must therefore take into account that (i) there are two different dynamic processes, with different free energies of activation; (ii) the lower barrier exchanges two of the three C_6F_5 rings, leaving the third one (apparently) unaffected; (iii) the higher barrier exchanges the signals of all three rings.

The lower barrier observed in **1** could be explained in terms of a ring-flip mechanism involving a two-blade propeller (see Scheme 2), but in the present case the behavior of the third C_6F_5 ring (indicated as C in Figure 1) must also be taken into account. Indeed, if the lower barrier were due to a ring-flip mechanism involving only rings A and B, the two corresponding para fluorine atoms would not exchange their environment, in contrast with the experimental evidence.

A possible explanation for the spectra observed at lower temperature is that rings A and B undergo a two-ring-flip pathway; after that ring A moves over the triazole system, reaching the threshold transition state (TS in Scheme 3). Finally,

rings A and C undergo a one-ring-flip process that leads to the enantiomer of the starting conformer. By means of this mechanism the two rings involved in the two-blade propeller changed from being A−B to being A−C, while ring B becomes C and vice versa.

By applying this approach we deduce that four ortho fluorine atoms (those belonging to rings B and C) must exchange their positions, while the remaining two (those belonging to ring A) remain unchanged, since ring A is not involved in a 180° rotation around the B−C bond, but only in a 60° rotation.[22] As far as the para fluorines are concerned, two of them must exchange, while the signal of the third one (on ring A) should be unaffected. This corresponds exactly to the spectra observed at lower temperature and accounts for the energy barrier of 10.7 ± 0.2 kcal mol^{-1}. A similar multistep stereomutation mechanism was proposed in the case of triarylboranes.[12b,23,24]

The higher energy process exchanging all three rings can be easily interpreted by assuming a 120° rotation around the B−N bond. When this rotation is fast, the three rings lose their identity and a single line is observed for all the ortho, meta, and para fluorine signals, as experimentally observed when the sample of **1** was warmed to +75 °C in $C_2D_2Cl_4$ (see Figures 3 and 4).

This quite complicated mechanism finds additional experimental support by analysis of other dynamic NMR data obtained for similar compounds. It is found that the lower barrier value increases when the central nitrogen of benzotriazole is replaced by a CH group, as in benzimidazole[8] ($\Delta G^{\ddagger} = 13.0$ kcal mol^{-1}) and indole[3] ($\Delta G^{\ddagger} = 14.9$ kcal mol^{-1}), or a C-Me group, as in 2-methylindole[3] ($\Delta G^{\ddagger} = 18.4$ kcal mol^{-1}). This can be explained by the fact that in the proposed low-energy enantiomerization pathway the barrier is generated mainly by the steric hindrance caused by the ortho fluorine atom on ring A passing over the central nitrogen of the benzotriazole. When the lone pair of that nitrogen is replaced by a hydrogen or a methyl group, it is expected that the enantiomerization barrier will be increased.

In the case of adduct **2** we observed the same experimental behavior previously described for **1**, the two energy barriers

(21) To account for the proposed mechanism, in the case of the ortho signals only selected rate constants have to be considered, since the enantiomerization process exchanges a single ortho signal of the two C_6F_5 rings into a signal of the other ring, but it does not exchange the two ortho fluorine signals belonging to the same ring. Thus k_{25} and k_{36} are related to the enantiomerization process and they exchange the second with the fifth line and the third with the sixth, respectively, while k_{16} and k_{45} are related to the B−N rotation process and they exchange the first with the sixth line and the fourth with the fifth, respectively.

(22) The other possibility, i.e., a one-ring flip between A and B, would require a transition state in which ring A is orthogonal to the benzotriazole ring; this would imply the exchange between the two ortho fluorine signals of ring A, in contrast with the experimental evidence.

(23) Due to the huge molecular complexity, we did not attempt to calculate the full equilibration pathway for compound **1**. Therefore we could not completely exclude the possibility of a single concerted transition state for the enantiomerization process. In this case, however, the transition state would also correspond to the passage of one ortho fluorine of ring A over the benzotriazole.

(24) Finocchiaro, P.; Gust, D.; Mislow, K. *J. Am. Chem. Soc.* **1973**, *95*, 7029−7036.
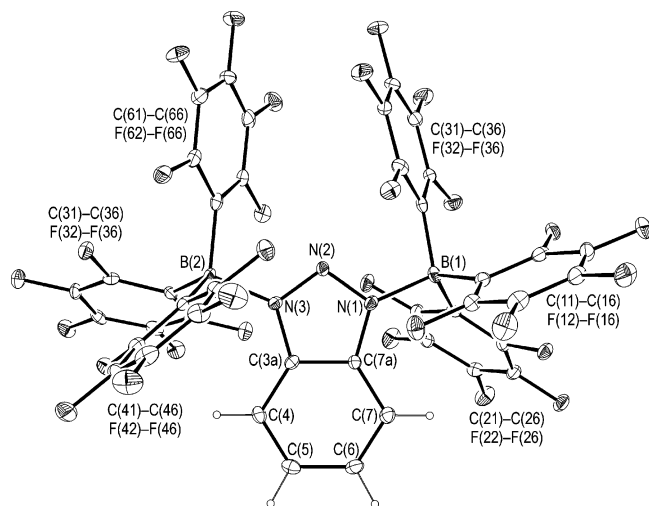
Figure 5. ORTEP view of the molecular structure of adduct **3** in the crystal.

being 11.0 ± 0.2 and 12.4 ± 0.2 kcal mol^{-1}. These values are very similar to the corresponding values observed for **1**. This shows that the effects of the different charge distribution in the benzotriazole ring of **1** and **2** on the enantiomerization barrier are extremely small.

In the case of the bis-susbstitued benzotriazole adduct **3**, the presence of the two elements of conformational chirality (i.e., the two helical two-blade propellers) can lead, in principle, to two conformational diastereoisomers (Figure 5), generated by the lower barrier enantiomerization process.

The structure of the hexakis(pentafluorophenyl)-$1\kappa^3$C,$2\kappa^3$C-μ-(1H-benzotriazolato-$1\kappa N^1$:$2\kappa N^3$) diborate anion **3** has been determined in the solid state by X-ray diffraction. Figure 5 shows a view of one of the two independent anions in the asymmetric unit of [NHEt$_3$]**3**·1/2C$_7$H$_8$, while Table 1 contains a list of some dihedral angles for **3** and other related compounds.

The formulation of **3** as an adduct between the benzotriazolate anion and two tris(pentafluorophenyl)borane groups is confirmed. The versatile triazolate anions, due to the presence of three basic nitrogen atoms, show a rich coordination chemistry,[25] acting either as a terminal ligand (with both coordination modes κN^1 and κN^2) or as a two- or three-center bridging ligand (μ-κN^1:κN^2, μ-κN^1:κN^3, and μ_3-κN^1:κN^2:κN^3).

In the asymmetric unit of [NHEt$_3$]**3**·1/2C$_7$H$_8$ two independent anions are present. As can be inferred by data given in Table S2 (see Supporting Information), they show an almost identical molecular geometry (the root-mean-square deviation between the two moieties is 0.255 Å). Both anions have an idealized C_2 symmetry, in accordance with the computed geometry for anion **3** at the HF/6-31G level of theory (see below). The average bonding parameters for anion **3** agree well with the corresponding values observed for similar benzotriazolato ligands.[26]

As previously stated,[3] the two B(C$_6$F$_5$)$_3$ moieties adopt a very similar conformation. In particular, one of the three phenyl rings, the so-called "in-plane" ring labeled C(11)−C(16) and C(31)−C(36), almost eclipses the B−N bond, whereas the other two exhibit the two-blade propeller conformation. This conformation can be found in most of the crystal structures of tris(pentafluorophenyl)borane derivatives.[18] It must be noted that this arrange-

ment of the pentafluorophenyl rings does not seem to be a consequence of the formation of any particular nonbonded or hydrogen-bonded interaction between the B(C$_6$F$_5$)$_3$ moiety and the rest of the molecule, since it can be observed even in adducts with sterically undemanding ligands not bearing any acidic hydrogen atoms, as is the case here.

Ab initio calculations show that also in an isolated molecule of **3** the two B(C$_6$F$_5$)$_3$ moieties show the same two-blade helical conformation and that two energy minima, corresponding to two diastereoisomers arising from the relative positions of the two B(C$_6$F$_5$)$_3$ groups, are present (Figure 6). The lower energy diastereoisomer has C_2 symmetry, while the second one has C_s symmetry, and it is calculated to be 1.69 kcal mol^{-1} less stable at the HF/6-311+G(d)//HF/6-31G level of theory.[17]

The ^{19}F spectrum of **3** obtained at −75 °C shows a total of 28 signals of different intensity, indicating the presence of the two expected diastereoisomers. In particular, three pairs of signals in an 80:20 proportion are visible in the para fluorine region of the spectrum (Figure 7). On raising the temperature, two major signals and two minor signals begin to show line-broadening effects due to the first dynamic process, the free energy of activation being 11.7 ± 0.2 kcal mol^{-1} (k_d in Figure 7). It is worth noting that this energy barrier is very similar to that obtained for the enantiomerization process in **1** and **2**. This observation further supports the proposed mechanism for the low-energy interconversion because the two diastereoisomers of **3** can interconvert by the exchange of the internal conformation of a single B(C$_6$F$_5$)$_3$ moiety.

As in many other cases of conformational equilibria in solution, only the more stable conformation is usually present in the crystalline state. In this case the crystal contains only the C_2 isomer, so the same symmetry can be confidently assigned to the major diastereoisomer in solution. This assignment is also supported by the ab initio calculation.

In further ^{19}F NMR experimental observations on **3** the second dynamic process that exchanges all para fluorine signals was shown to take place when the temperature is raised above −27 °C, and a single signal was observed at +25 °C ($\Delta G^{\ddagger} = 12.5 \pm 0.5$ kcal mol^{-1}, k_r in Figure 7).[27]

Conclusions

In conlusion, two different energy barriers corresponding to an enantiomerization process and a B−N rotation were observed in a class of tris(pentafluorophenyl)borane−benzotriazole adducts. The lower barrier enantiomerization pathway has been interpreted by a complex three-step process involving all the perfluorinated rings. The higher energy process has been assigned to the rotation of the whole tris(pentafluorophenyl)borane moiety around the B−N bond. In the case of the bis-adduct **3**, two conformational diastereoisomers with different populations were detected at low temperature.
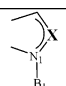
Experimental Section

General Procedures and Starting Materials. All operations were performed under nitrogen by using conventional Schlenk-line techniques. Solvents were purified by degassing with N$_2$ and passing over activated (8 h, N$_2$ purge, 300 °C) Al$_2$O$_3$, and stored under nitrogen. Benzotriazole (Aldrich, purity 98%), NEt$_3$ (Aldrich,

(25) Moore, D. S.; Robinson, S. D. *Adv. Inorg. Chem.* **1988**, *32*, 171−239, and references therein.

(26) Mean bond distances (Å) for the benzotriazolato ligand are as follows: N−N 1.334, N−C 1.366, C(3a)−C(7a) 1.393, C(3a)−C(4) 1.405, C(4)−C(5) 1.368, C(5)−C(6) 1.407.

(27) In this case only a rough evaluation of the free energy of activation was obtained, because of the large line broadening due to very fast T_2 relaxation induced by the quadrupolar effect of the two boron atoms. This broadening is much less marked when only one boron atom is present, like in **1** and **2**.

Table 1. Experimental Energy Barriers (kcal mol⁻¹) and Dihedral Angles (deg) for 1−3 and Some Related Compounds

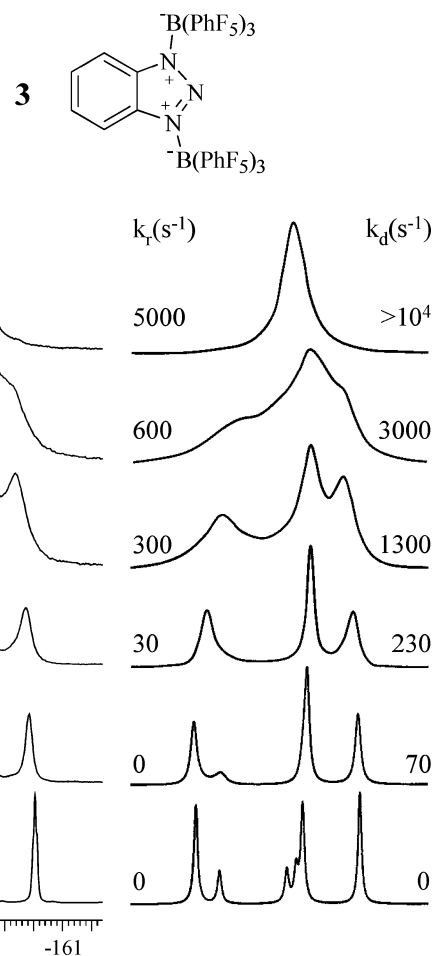| compd	heterocycle	X	$\Delta G^{\ne}$ B–C rotation	$\Delta G^{\ne}$ B–N rotation	N(1)–B(1)–C–C			X–N(1)–B(1)–C		
1	Benzotriazole	N	10.7	12.8						
2	Benzotriazole	N	11.0	12.4						
3	Benzotriazole	N	11.7	12.5	−9.2[a]	57.5[a]	59.5[a]	119.2[a]	−117.9[a]	3.3[a]
Ref. 8	Benzimidazole	CH	13.0	15.9	−15.0	63.2	57.0	119.8	−115.9	4.8
Ref. 3	Indole	CH	14.9	16.7	−17.8	67.3	53.3	129.6	−106.7	14.5
Ref. 3	2-Methylindole	C-Me	18.4	–						

[a] Average values.
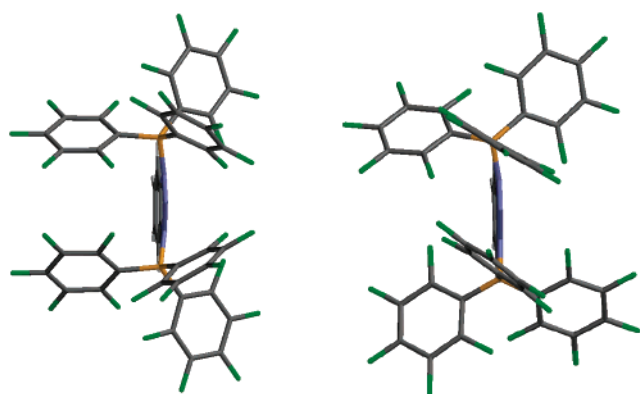
Figure 6. Optimized structure (HF/6-311+G(d)//HF/6-31G) of the C_s diastereoisomer (left) and the C_2 diastereoisomer (right) of **3**.

purity 99.5%), and B(C₆F₅)₃ (Boulder) were used as received. Mass spectra were recorded from acetonitrile solutions by the electron spray ionization (ESI⁺ and ESI⁻) method.

NMR Measurements. The ¹H, ¹³C, and ¹⁹F NMR spectra were recorded on a spectrometer equipped with a dual switchable direct probe, operating at 600, 150.8, and 564.3 MHz, respectively. The samples were dissolved in CDCl₃, CD₂Cl₂, or toluene-d_8. As reference, the residual peak of CHCl₃, CHDCl₂, and CHD₂C₆D₅ in the ¹H spectra (7.27, 5.35, and 2.15 ppm, respectively), the peak of the solvent in the ¹³C spectra (77.7 ppm for CDCl₃, 54.20 ppm for CD₂Cl₂, and 20.4 for toluene-d_8), and the external standard C₆F₆ (−163.0 ppm) in the ¹⁹F spectra were used. The samples for the low-temperature measurements were prepared under a nitrogen atmosphere and subsequently sealed. The temperatures were calibrated by substituting the sample with a precision Cu/Ni thermocouple before the measurements. Complete fitting of dynamic NMR line shapes was carried out using a PC version of the DNMR-6 program.[28] At least five different temperature spectra were used for the simulations.

3-[Tris(pentafluorophenyl)borane]-1H-benzotriazole (1). Benzotriazole (0.51 g, 4.2 mmol), previously dissolved in 8 mL of dichloromethane, was added at room temperature to a suspension of B(C₆F₅)₃ (2.19 g, 4.2 mmol) in 10 mL of dichloromethane to give a yellow solution. After 20 min of stirring at rt, the solvent was removed under reduced pressure to give a white-gray solid in quantitative yield: MS (ESI) (rel int) 630 (M − 1)⁻ (100), 629 (25); ¹H NMR (CD₂Cl₂) δ 7.56 (1 H, ddd, J = 8.75, 6.95, and 1.05 Hz), 7.63 (1 H, dt, J = 8.75 and 0.95 Hz), 7.71 (1 H, ddd, J = 8.60, 6.95, and 0.95 Hz), 7.87 (1 H, ddd, J = 8.60, 1.05, and 0.95 Hz); ¹³C NMR (CD₂Cl₂, ¹⁹F and ¹H decoupled) δ 113.22 (CH), 116.44 (CH), 118.21 (Cq, br, C−B), 129.91 (CH), 131.06 (CH), 134.35 (Cq), 137.84 (Cq-F, *meta*), 138.91 (Cq), 140.95 (Cq-F, *para*), 149.04 (Cq-F, br, *ortho*); ¹⁹F NMR (CD₂Cl₂) δ −164.0 (*meta*), −157.2 (*para*), −136 to −124 (broad signals, *ortho*). Anal.

(28) *PC version of the QCPE program no. 633*; Indiana University: Bloomington, IN.

3

T(°C)	k_r(s⁻¹)	k_d(s⁻¹)
+25	5000	>10⁴
+3	600	3000
-7	300	1300
-27	30	230
-36	0	70
-80	0	0

-157　　　　-159　　　　-161

Figure 7. Left: temperature dependence of the para region of the ¹⁹F NMR signals of compound **3** (564.3 MHz in CD₂Cl₂). Right: line shape simulations obtained with the rate constants indicated.

Calcd for C₂₄H₅BF₁₅N₃: C, 45.68; H, 0.80; N, 6.66. Found: C, 45,52; H, 0.98; N, 7.01.

Triethylammonium 1-[Tris(pentafluorophenyl)borane]-1H-benzotriazole (2). Triethylamine (0.22 g, 2.1 mmol) was added to a solution of adduct **1** (1.35 g, 2.1 mmol) in 15 mL of dichloromethane. After 1 h of stirring at rt, the solvent was evaporated under reduced pressure, and compound **2** was isolated as a light yellow solid in quantitative yield: MS (ESI) (rel int) 630 (M borate moiety)⁻ (100), 629 (25), and 102 (M ammonium)⁺; ¹H NMR (CD₂Cl₂) δ 1.29 (t, 9 H, Me, J = 7.6 Hz), 3.11 (q, 6 H, CH₂, J = 7.6 Hz), 7.18−7.26 (m, 2 H), 7.32 (d, 1 H, J = 8.0 Hz), 7.76 (1 H, dt, J = 8.75 and 1.3 Hz); ¹³C NMR (CD₂Cl₂, ¹⁹F and ¹H decoupled) δ 9.21 (Me), 47.41 (CH₂), 114.27 (CH), 117.49 (CH), 121.26 (Cq, br, C-B), 124.25 (CH), 126.22 (CH), 137.50 (Cq-F, *meta*), 138.79 (Cq), 140.01 (Cq-F, *para*), 145.24 (Cq), 149.05 (Cq-F, br, *ortho*); ¹⁹F NMR (CD₂Cl₂) δ −165.4 (*meta*), −159.7 (*para*), −136 to −124

(broad signals, *ortho*). Anal. Calcd for $C_{30}H_{20}BF_{15}N_4$: C, 49.20; H, 2.75; N, 7.65. Found: C, 49.50; H, 2.95; N, 7.48.

Triethylammonium 1,3-Bis[tris(pentafluorophenyl)borane]-1*H*-benzotriazole (3). A solution of salt **2** (0.32 g, 0.44 mmol) in 8 mL of dichloromethane was added to a suspension of $B(C_6F_5)_3$ (0.22 g, 0.43 mmol) in 2 mL of dichloromethane. After removal of the solvent under reduced pressure, product **3** was isolated as a whitish solid after 4 h stirring at room temperature (yield = 92%): MS (ESI) (rel int) 1142 (M diborate moiety)$^-$ (100), 1141 (40), and 102 (M ammonium)$^+$; ^{1}H NMR (CD$_2$Cl$_2$) δ 1.36 (t, 9 H, Me, $J = 7.5$ Hz), 3.24 (q, 6 H, CH$_2$, $J = 7.5$ Hz), 4.96 (1 H, br t, N-*H*), 7.24 (m, 2 H), 7.30 (s, 1 H), 7.31 (m, 2 H); ^{13}C NMR (CD$_2$Cl$_2$, ^{19}F and ^{1}H decoupled) δ 10.11 (Me), 49.70 (CH$_2$), 115.36 (CH), 119.75 (Cq, br, C-B), 127.20 (CH), 137.44 (Cq-F, *meta*), 139.51 (Cq), 140.37 (Cq-F, *para*), 149.01 (Cq-F, br, *ortho*); ^{19}F NMR (CD$_2$Cl$_2$) δ -166.1 (*meta*), -159.8 (*para*), -137 to -123 (broad signals, *ortho*). Colorless crystals suitable for X-ray diffraction analysis were isolated from a toluene solution stored at -20 °C for 5 days. Anal. Calcd for $C_{48}H_{20}B_2F_{30}N_4$: C, 46.33; H, 1.62; N, 4.50. Found: C, 46.55; H, 1.86; N, 4.67.

Triethylammonium 1,3-Bis[tris(pentafluorophenyl)borane]-1*H*-benzotriazole (3) (experiment in one step). A mixture of benzotriazole (0.28 g, 2.35 mmol) and $B(C_6F_5)_3$ (2.41 g, 4.7 mmol) in dichloromethane was stirred for 2 h at room temperature, and then a solution of triethylamine (0.24 g, 2.37 mmol) in dichloromethane was added. ^{1}H NMR analysis showed the formation of adduct **3** together with 10% of compound **1**, which was easily removed by washing the crude with chloroform, since **3** has a very low solubility in this solvent. Compound **3** was obtained as a pure white solid (88%).

The corresponding dioctadecylmethylammonium salt was previously prepared in 70% yield by refluxing benzotriazole, $B(C_6F_5)_3$, and dioctadecylmethylamine in toluene.[9]

X-ray Structural Analysis. Crystal data for [NHEt$_3$]**3**·1/2C$_7$H$_8$: $C_{51.5}H_{24}B_2F_{30}N_4$, $M_r = 1290.37$, triclinic, space group $P\bar{1}$ (No. 2), $a = 12.640(3)$ Å, $b = 23.317(6)$ Å, $c = 19.605(4)$ Å, $\alpha = 108.66(1)°$, $\beta = 97.26(1)°$, $\gamma = 108.29(1)°$, $V = 5030(2)$ Å^3, $Z = 4$, $T = 100(2)$ K, graphite-monochromated Mo Kα radiation ($\lambda = 0.71073$ Å), $\rho_{calcd} = 1.704$ g cm^{-3}, $F(000) = 2564$, colorless crystal, μ(Mo Kα) = 0.178 mm^{-1}, empirical absorption correction (SAD-ABS,[29] 13 604 symmetry-equivalent reflections, average redundancy 2.6, effective data-to-parameter ratio 4.6), minimum relative transmission factor 0.900, Bruker SMART diffractometer, ω scans

($\Delta\omega = 0.3°$), 2400 frames each at 30 s of exposure, keeping the detector at 4.5 cm from the sample, $1.0° \leq \theta \leq 25.1°$, index ranges $h = -15 \rightarrow 15$, $k = -23 \rightarrow 23$, $l = -27 \rightarrow 27$, 40 015 reflections of which 17 651 were unique ($R_{int} = 0.0338$, $R_\sigma = 0.0238$), 14 035 reflections with $I > 2\sigma(I)$, no intensity decay, solution by direct methods (SIR97[30]) and subsequent Fourier synthesis, anisotropic full-matrix least-squares on F^2 using all reflections (SHELX97[31]), hydrogen atoms placed in idealized position, data/parameters 17 651/1576, $S(F^2) = 1.000$, $R[F, I > 2\sigma(I)] = 0.0319$, $wR(F^2$, all data) = 0.0798, weighting scheme $w = 1/[\sigma^2(F_o^2) + (0.05P)^2 + 0.6P]$, where $P = (F_o^2 + 2F_c^2)/3$, maximum/minimum residual electron density 0.206/-0.205 e Å^{-3}.

Crystallographic data (excluding structure factors) for adduct **3** have been deposited with the Cambridge Crystallographic Data Centre as supplementary publication no. 279031. Copies of the data can be obtained free of charge on application to the CCDC, 12 Union Road, Cambridge CB2 1EZ, UK (fax, (+44)1223/336033; e-mail, deposit@ccdc.cam.ac.uk).

Computations. Geometry optimizations were carried out at the HF/6-31G level by means of Gaussian 03.[17] The standard Berny algorithm in redundant internal coordinates and default criteria of convergence were employed. Harmonic vibrational frequencies were calculated in order to ascertain the nature of all the stationary points. For each optimized structure no imaginary frequencies were found. For compound **3**, single-point energies were subsequently calculated at the HF/6-311+G(d) level.

Supporting Information Available: Data for the homopolymerization of 1-hexene; ORTEP views of the two independent anions in the crystal structure of [NHEt$_3$]**3**·1/2C$_7$H$_8$; selected geometric parameters for **3**; computational data for **1** and **3**. This material is available free of charge via the Internet at http://pubs.acs.org.

OM051003T

(29) Sheldrick, G. M. *SADABS*; Universität Göttingen: Germany, 1996.

(30) Altomare, A.; Burla, M. C.; Camalli, M.; Cascarano, G. L.; Giacovazzo, C.; Guagliardi, A.; Moliterni, A. G. G.; Polidori, G.; Spagna, R. *J. Appl. Crystallogr.* **1999**, *32*, 115−119.

(31) Sheldrick, G. M. *SHELX97*; Universität Göttingen: Germany, 1997.